

## A 'sliding contact' dynamic force spectroscopy method for interrogating slowly forming polymer crosslinks.

Kate Alexandra Bowman, Olav Andreas Aarstad, Bjørn Torger Stokke, Gudmund Skjåk-Bræk, and Andrew N. Round

*Langmuir*, **Just Accepted Manuscript** • DOI: 10.1021/acs.langmuir.6b03414 • Publication Date (Web): 04 Nov 2016

Downloaded from <http://pubs.acs.org> on November 7, 2016

### Just Accepted

"Just Accepted" manuscripts have been peer-reviewed and accepted for publication. They are posted online prior to technical editing, formatting for publication and author proofing. The American Chemical Society provides "Just Accepted" as a free service to the research community to expedite the dissemination of scientific material as soon as possible after acceptance. "Just Accepted" manuscripts appear in full in PDF format accompanied by an HTML abstract. "Just Accepted" manuscripts have been fully peer reviewed, but should not be considered the official version of record. They are accessible to all readers and citable by the Digital Object Identifier (DOI®). "Just Accepted" is an optional service offered to authors. Therefore, the "Just Accepted" Web site may not include all articles that will be published in the journal. After a manuscript is technically edited and formatted, it will be removed from the "Just Accepted" Web site and published as an ASAP article. Note that technical editing may introduce minor changes to the manuscript text and/or graphics which could affect content, and all legal disclaimers and ethical guidelines that apply to the journal pertain. ACS cannot be held responsible for errors or consequences arising from the use of information contained in these "Just Accepted" manuscripts.



1  
2  
3 1 **A ‘sliding contact’ dynamic force spectroscopy method for interrogating slowly forming**  
4 **polymer crosslinks.**  
5  
6  
7 3

8  
9 4 Kate A. Bowman<sup>1</sup>, Olav Andreas Aarstad<sup>2</sup>, Bjørn Torger Stokke<sup>3</sup>, Gudmund Skjåk-Bræk<sup>2</sup>  
10 and Andrew N. Round<sup>1</sup>  
11

12 1 University of East Anglia, School of Pharmacy (United Kingdom); 2 Norwegian University  
13 of Science and Technology, Department of Biotechnology (Norway); 3 Norwegian  
14 University of Science and Technology, Department of Physics  
15  
16  
17 9

18  
19 10 **Abstract**

20  
21 11 Dynamic Single Molecule Force Spectroscopy (SMFS), conducted most commonly using  
22 AFM, has become a widespread and valuable tool for understanding the kinetics and  
23 thermodynamics of fundamental molecular processes such as ligand-receptor interactions and  
24 protein unfolding. Where slowly forming bonds are responsible for the primary  
25 characteristics of a material, as is the case in crosslinks in some polymer gels, care must be  
26 taken to ensure that a fully equilibrated bond has first formed before its rupture can be  
27 interpreted. Here we introduce a method, sliding contact force spectroscopy (SCFS), which  
28 effectively eliminates the kinetics of bond formation from the measurement of bond rupture.  
29 In addition it permits bond rupture measurements in systems where one of the binding  
30 partners may be introduced into solution prior to binding without tethering to a surface.  
31 Taking as an exemplar of a slowly forming bond the ‘eggbox’ junction crosslinks between  
32 oligoguluronic acid chains (oligoGs) in the commercially important polysaccharide alginate,  
33 we show that SCFS measures accurately the equilibrated bond strength of the crosslink when  
34 one chain is introduced into the sample solution without tethering to a surface. The results  
35 validate the SCFS technique for performing single molecule force spectroscopy experiments,  
36 and show that it has advantages in cases where the bond to be studied forms slowly and  
37 where tethering of one of the binding partners is impractical.  
38  
39  
40  
41  
42  
43  
44  
45  
46  
47  
48  
49  
50  
51  
52  
53  
54  
55  
56  
57  
58  
59  
60

28  
29 11 **Introduction**

30 The nature of the dynamic single molecule force spectroscopy (SMFS) experiment allows  
31 inherent variations in individual trajectories of unbinding to be observed directly and in real  
32 time, while the kinetics and, more recently, the thermodynamics of the bond rupture can be  
33 measured<sup>1</sup>. This ability has been widely applied in the study of the rupture of bonds ranging  
34 from ligand-receptor interactions to the bonds holding proteins in their folded state. To

1  
2  
3 35 characterise a bond formed between two initially separated binding partners, such as that  
4  
5 36 between a ligand and a receptor, the SMFS experiment typically involves tethering the two  
6  
7 37 binding partners to the two surfaces involved (a substrate and the force transducing probe),  
8  
9 38 typically by a polyethylene glycol (PEG) chain. The two surfaces are then brought together  
10  
11 39 for a short time (typically milliseconds, during which the bond between the ligand and  
12  
13 40 receptor may form) and then separated, whereupon the bond is broken. The record of the  
14  
15 41 force experienced by the probe as it is separated from the substrate constitutes the raw data  
16  
17 42 for the dynamic force spectrum (DFS), which is then constructed from a plot of rupture  
18  
19 43 forces  $f$  at (the natural log of) instantaneous loading rates at rupture  $r$ . Kinetic and  
20  
21 44 thermodynamic parameters are then extracted from fits to the plot of  $f$  vs.  $\ln(r)$ . For nearly  
22  
23 45 two decades the prevailing model for ligand-receptor interactions measured by SMFS has  
24  
25 46 been the Bell-Evans model<sup>2</sup>, which characterises rupture bonds in terms of  $k_{\text{off}}$  and  $x_{\text{t}}$ , the  
26  
27 47 kinetic off rate and the distance to the transition state barrier, but recently a new model<sup>3</sup> has  
28  
29 48 been developed that seamlessly combines the slow and fast loading rate regimes and allows  
30  
31 49 extraction of the thermodynamic parameter  $\Delta G_{\text{bu}}$ , the free energy of unbinding, as well as the  
32  
33 50 values of  $k_{\text{off}}$  and  $x_{\text{t}}$ .

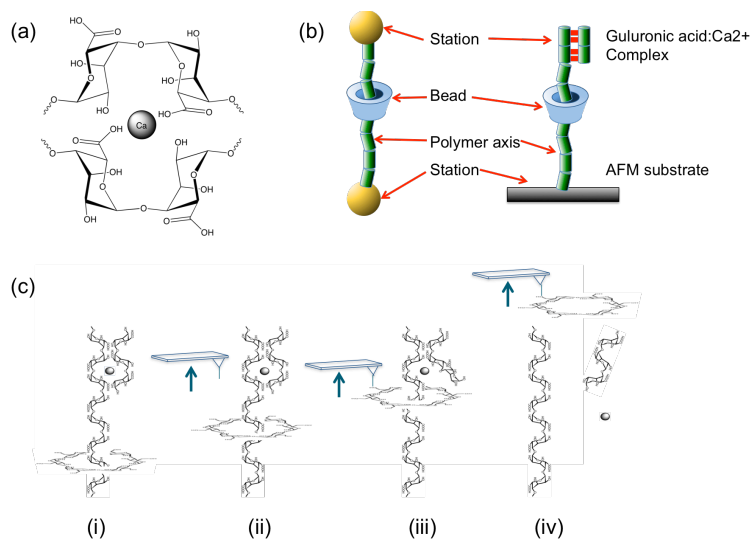
34 51  
35 52 Despite the technique relying on the measurement of bonds formed during short, millisecond-  
36  
37 53 timescale contacts between the two surfaces, measurements of the rate of bond formation are  
38  
39 54 confounded by the influence of probe dynamics and the elasticity of the tethers, so estimates  
40  
41 55 of  $k_{\text{on}}$  derived from AFM force spectroscopy measurements, while sometimes agreeing with  
42  
43 56 bulk measurements<sup>4</sup>, in other cases differ widely from those reported by other methods,  
44  
45 57 making it difficult to assess whether an equilibrated bond has formed. An example of this is  
46  
47 58 the case of the interaction between the antibiotic vancomycin and its target in *Staphylococcus*  
48  
49 59 *aureus*, the D-Ala- D-Ala terminus of the bacterial cell wall peptidoglycan precursor<sup>5</sup>.  
50  
51 60 Isothermal calorimetry<sup>6,7</sup>, affinity capillary electrophoresis<sup>8</sup> and competitive titration  
52  
53 61 methods<sup>9</sup> have previously established that the dissociation constant  $K_{\text{D}}$  for this interaction is  
54  
55 62 in the range of  $1 \times 10^{-6} - 10^{-9}$  M, whereas AFM analysis<sup>4</sup> produced values of  $k_{\text{off}}$  and  $k_{\text{on}}$  of  
56  
57 63  $2 \times 10^{-3} \text{ s}^{-1}$  and  $5 \text{ M}^{-1} \text{ s}^{-1}$  respectively, giving a value for  $K_{\text{D}}$  of 0.4 mM; a difference of 3-6  
58  
59 64 orders of magnitude from the range of bulk solution values. Given that typical  $k_{\text{on}}$  values for  
60  
61 65 ligand-receptor interactions such as vancomycin- D-Ala- D-Ala are of the order of  $10^6$  or  $10^7$   
62  
63 66  $\text{M}^{-1} \text{ s}^{-1}$ <sup>10</sup> rather than the  $5 \text{ M}^{-1} \text{ s}^{-1}$  measured by AFM, it is clear that estimates of  $k_{\text{on}}$  based on  
64  
65 67 AFM data can be inaccurate. Consequences arising from the conditions inherent in

1  
2  
3 68 conventional single molecule force spectroscopy therefore include a suboptimal sampling of  
4  
5 69 slowly formed bonds due to the limited time available for bonds to be formed.  
6  
7 70

8  
9 71 In many cases studied, the high  $k_{\text{on}}$  typical for ligand-receptor interactions allows us to  
10  
11 72 assume that fully equilibrated bonds form during the tens of milliseconds that probe and  
12  
13 73 substrate are close together during a force spectroscopy cycle. However, an example of an  
14  
15 74 important interaction for which the limited time for bond formation may affect SMFS  
16  
17 75 measurements is the calcium-mediated ‘eggbox’ junction, crosslinking between sequences of  
18  
19 76 oligoguluronic acids (oligoGs), that is primarily responsible for alginate gelation. Each unit  
20  
21 77 of an eggbox junction consists of a calcium ion-mediated interaction between pairs of  
22  
23 78 guluronic acids (gulA) on opposing chains of alginate in a 2:1:2 gulA:Ca<sup>2+</sup>:gulA complex  
24  
25 79 (Figure 1a). Consecutive sequences of these interactions constitute the eggbox junction,  
26  
27 80 forming a crosslink in the network. The rheology of polymer gels is strongly influenced by  
28  
29 81 long timescale relaxation processes that occur following formation and deformation of the  
30  
31 82 gel<sup>11-13</sup>. These relaxation processes, which can take hours to complete, involve the breaking  
32  
33 83 and reforming of the interactions underpinning these crosslinks to resolve internal stresses  
34  
35 84 arising from the deformation. Recently<sup>14</sup> we showed that even at the level of individual  
36  
37 85 crosslinks, in oligoGs as short as 16 units, times of several hundred milliseconds were  
38  
39 86 required for the crosslinks to reach their equilibrated, full strength. This poses a problem for  
40  
41 87 the study of crosslinking at the molecular level using techniques such as atomic force  
42  
43 88 microscopy (AFM)-based single molecule dynamic force spectroscopy (SMFS) since as  
44  
45 89 dwell times of the probe at the substrate increase, the incidence of multiple and non-specific  
46  
47 90 interactions increase, potentially obscuring the specific interactions of interest and leading to  
48  
49 91 inaccurate measurements. Recently this problem was shown to be especially acute for  
50  
51 92 binding partners coupled to long tethers<sup>15</sup>. Conversely, the use of long tethers make the  
52  
53 93 identification of single bond ruptures possible on the basis of the apparent Kuhn length of the  
54  
55 94 PEG tether<sup>16</sup>. Indeed, in the study described above we were unable to extend the analysis of  
56  
57 95 the bond rupture beyond 500 ms due to the paucity of reliable specific, single bond ruptures  
58  
59 96 at longer dwell times. A single molecule method that allows the accurate measurement of the  
60  
61 97 strength of equilibrated crosslinks within polymer chains is, therefore, lacking.  
62  
63 98

58 99 An alternative iteration of dynamic force spectroscopy may be called ‘sliding contact’  
59  
60 100 (dynamic) force spectroscopy (hereafter SCFS). The SCFS method (Figure 1b) introduces a  
61  
62 101 ‘sliding contact’ between the AFM probe and the substrate, formed by a (pseudo)rotaxane<sup>17</sup>.

1  
2  
3  
4 102 A rotaxane consists of a macrocyclic ‘bead’ threaded onto a polymer axis, with ‘stations’ or  
5 103 ‘stoppers’ along the axis that interact with the bead or stop it from sliding off the end of the  
6  
7 104 polymer axis (the presence or absence of stoppers distinguishes a rotaxane from a  
8  
9 105 pseudorotaxane)<sup>18</sup>. In SCFS, the polymer axis will be the polymer of interest conjugated to a  
10 106 poly(ethylene glycol) (PEG) polymer, on to which a bead ( $\alpha$ -cyclodextrin (CD), with a tether  
11  
12 107 terminating in a reactive group recognised by the AFM probe) is threaded. The spontaneous  
13  
14 108 formation of polyrotaxanes between PEG and  $\alpha$ -CD is well known<sup>17,18</sup>, whereby the PEG  
15  
16 109 threads into the pore of the  $\alpha$ -CD. The PEG is grafted to a substrate suitable for SMFS that  
17  
18 110 acts as a stopper, and the AFM probe is brought into contact with the substrate and retracted,  
19  
20 111 as in a conventional SMFS experiment. When a bond is formed between the AFM probe and  
21  
22 112 the tether on the CD and the probe retracts, the CD is forced to slide along the polymer axis,  
23  
24 113 encountering resistance to sliding in proportion to the strength of the interaction between the  
25  
26 114 CD bead and the polymer axis, station or stopper it encounters. This change in resistance will  
27  
28 115 be recorded in the force vs. separation spectrum in the same way as other changes in force  
29  
30 116 (such as polymer stretching and bond rupture) are in conventional DFS. In the present work,  
31  
32 117 the complex formed by the two guluronic acid oligomers and  $\text{Ca}^{2+}$  ions represents a station  
33  
34 118 and the process that occurs when the CD bead encounters this complex is sketched in figure  
35  
36 119 1c. A similar dynamic force spectrum can be constructed and the same models used to fit the  
37  
38 120 data and characterise the sliding of the CD over a station or stopper. Iterations of this  
39  
40 121 approach have been used to manipulate  $\alpha$ -CD beads forming a polyrotaxane with PEG back  
41  
42 122 and forth along the PEG axle<sup>19</sup>, and to measure the force required to drive a bead between  
43  
44 123 two stations in a rotaxane<sup>20,21</sup>. It has also been considered as a potential sequencing tool for  
45  
46 124 DNA and other polymers<sup>22-25</sup>.



126

1  
2  
3 127  
4  
5 128 *Figure 1. (a) Structure of the 'eggbox' junction zone between two pairs of guluronic acid*  
6 *sequences and a divalent metal cation such as calcium. (b) diagram showing the analogy*  
7 129 *between a conventional rotaxane (left) and the sliding contact pseudorotaxane (right). The*  
8 *common features (stations, bead, axis) are labelled in each. (c) Illustration of the proposed*  
9 130 *mechanism of unzipping of an eggbox junction by sliding contact force spectroscopy. (i) A*  
10 131 *cyclodextrin macrocycle forms a pseudorotaxane with the PEG portion of a PEG-guluronic*  
11 132 *acid conjugate; (ii) an AFM probe binds to a tether on the cyclodextrin; (iii) the AFM probe*  
12 133 *retracts, pulling the tethered cyclodextrin along the conjugate; (iv) any guluronic acid*  
13 134 *oligomers bound to the conjugate are displaced by the cyclodextrin as it slides along.*  
14 135  
15 136  
16 137  
17  
18  
19  
20  
21  
22

23 138 While SCFS offers the opportunity to measure the difference in interaction between the  
24 139 sliding CD and the monomers in the polymer axle during sliding, the CD may also be used as  
25 140 a molecular 'zipper' to unzip molecules bound to sites incorporated into the polymer. From  
26 141 the point of view of addressing the eggbox junction zone in alginate, crosslinking between  
27 142 the oligoG conjugated to the PEG (and along which the CD is driven by the AFM probe) and  
28 143 untethered oligoG that has bound to it may be treated as a kind of stopper, in that the CD pore  
29 144 is too small to accommodate both strands and so proceeds by unzipping the interaction between  
30 145 the conjugated and untethered oligoG. This application of SCFS offers an alternative that  
31 146 potentially addresses several drawbacks of conventional DFS, including those highlighted  
32 147 above. Firstly, because the AFM probe is functionalised to pick up a tether attached to the  
33 148 functionalised CD and does not need to form the bond to be broken during the approach cycle  
34 149 of the experiment, SCFS offers the freedom to allow the bond of interest to be formed under  
35 150 ideal conditions and timescales. Secondly, once the CD has been picked up by the AFM  
36 151 probe, the retraction of the probe drives the CD along the polymer, so the direction of the  
37 152 unzipping action is controlled by the sequence and orientation of crosslinking sites along the  
38 153 polymer. Thirdly, only one of the binding partners needs to be tethered to the substrate,  
39 154 allowing the probing of interactions between a tethered and a free binding partner, removing  
40 155 a source of potential distortion of the interaction between the binding partners.  
41 156  
42  
43  
44  
45  
46  
47  
48  
49  
50  
51  
52  
53  
54  
55

56 157 Here we show that SCFS can be used to (i) break bonds formed between an untethered  
57 158 oligoguluronic acid chain (oligoG) and its tethered counterpart in the presence of free  $\text{Ca}^{2+}$ ,  
58 159 (ii) consider the effects the controlled direction of sliding has on the rupture of the bond, and  
59 160 (iii) establish the value of the free energy of unbinding  $\Delta G_{\text{bu}}$  of fully equilibrated crosslinks

1  
2  
3 161 between the two oligomers, where binding is estimated to take on the order of seconds to  
4  
5 162 reach full strength. We thereby aim to establish this method as a viable one for measuring the  
6  
7 163 equilibrated bond strength of slowly forming bonds at the single molecule level.  
8  
9 164

## 10 165 **Experimental**

11  
12 166

### 13 167 **OligoG conjugation, rotaxane formation and immobilisation**

14 168 Conjugates between purified oligoGs with  $n = 6, 10$  and 16-18 guluronic acid monomers and  
15  
16 169 PEG were prepared as described previously<sup>14</sup>. Briefly, oligoGs were end-functionalised with  
17  
18 170 Boc-NH-PEG-NH<sub>2</sub> (an amine-terminated poly(ethylene glycol) (PEG) with a *tert*-  
19  
20 171 butoxycarbonyl (Boc) protecting group) using a reductive amination method<sup>26</sup> previously  
21  
22 172 demonstrated for covalently linking polysaccharides to AFM probes and substrates<sup>27</sup>. The  
23  
24 173 deprotected amine group on the oligoG-PEG conjugate was coupled to a N-  
25  
26 174 hydroxysuccinimide-PEG-maleimide (NHS-PEG-Mal) and this conjugate was coupled to a  
27  
28 175 mica surface functionalised with thiol groups following a method previously used to  
29  
30 176 functionalise silica beads<sup>28</sup>.  $\alpha$ -cyclodextrins were modified with a bisamine-terminated PPG-  
31  
32 177 PEG-PPG tether as described previously<sup>23</sup>. Briefly, aldehyde groups were created on the  
33  
34 178 cyclodextrins by treatment with Dess-Martin periodinane and bis(2-aminopropyl)  
35  
36 179 polypropylene oxide-polyethylene oxide block copolymer was coupled to the aldehyde in a  
37  
38 180 Schiff base reaction. 0.4% w/w of each PEG-oligoG conjugate was mixed with a 1:1 mole  
39  
40 181 equivalent of amino-functionalized  $\alpha$ -CD for 24 hours, and deposited onto template-stripped  
41  
42 182 gold from water for 24 hours. Untethered oligoGs were used as isolated after purification.  
43

44 183  
44 184 AFM probes (MLCT silicon nitride from Veeco Instruments, Santa Barbara, CA, USA) with  
45  
46 185 nominal spring constants of 10 and 20 pN/nm were silanised with thiol-terminated alkylsilane  
47  
48 186 and then further functionalised with NHS-PEG-Mal as described above.  
49

### 50 187 51 188 **AFM force spectroscopy experiments**

52 189 Force spectroscopy experiments were carried out using a JPK Nanowizard III (JPK, Berlin,  
53  
54 190 Germany) in buffered aqueous solution. Spring constants (calibrated using the method built  
55  
56 191 in to the JPK AFM and based on the method devised by Hutter & Bechhoefer<sup>29</sup>) ranged from  
57  
58 192 13.3 to 40.4 pN/nm. Experiments were conducted in 20 mM MOPS (3-morpholinopropane-1-  
59  
60 193 sulfonic acid), with the addition of 2 mM CaCl<sub>2</sub> and/or 20 mM EDTA as described. Force

194 curves were collected in arrays of 32×32 data points over areas of 2×2 μm<sup>2</sup> at a relative  
 195 setpoint of 0.2 nN. The z-length was 200 nm, the approach and retract speeds were set at 500  
 196 nm.s<sup>-1</sup> and data was collected at a rate of 2048 samples.s<sup>-1</sup>. Force curves were exported and  
 197 analysed using JPK's data processing software (JPK instruments, DE, ver. 4.2.23). For single  
 198 chain sliding experiments events with total length in the interval 10-30 nm were selected and  
 199 terminal plateau length was identified and measured using the JPK software, while for the  
 200 unzipping experiments, the unbinding events (occurring at a frequency of <10% in all cases)  
 201 were fitted with an extended freely-jointed chain model and those events with fitted contour  
 202 lengths in the interval 10–40 nm were selected for analysis using the Friddle- Noy-De Yoreo  
 203 (F-N-Y) model<sup>1,3</sup> for the forced rupture of bonds using OriginPro™ (OriginLab, ver. 8.0724).  
 204 In **equation 1**, the F-N-Y model recognises that rebinding at slow loading rates represents an  
 205 equilibrated situation, reflected by the equilibrium force  $f_{eq}$ , and also reflects the Bell-Evans  $f$   
 206  $\sim \ln(r)$  relation<sup>2</sup> in the high loading rate regime. Besides estimating the values of the kinetic  
 207 parameters  $x_t$  and  $k_{off}$  (**equation 2**) in common with the Bell-Evans model, the F-N-Y model  
 208 allows the estimation of the free energy of unbinding  $\Delta G_{bu}$  for the single molecule interaction  
 209 from the values of  $f_{eq}$  and  $k_{eff}$ , the effective spring constant (**equation 3**).

210

211 *Equation 1.*

$$\langle f \rangle = f_{eq} + f_{\beta} \cdot \ln \left( 1 + e^{-0.577} \cdot \frac{r}{f_{\beta} k_u(f)} \right)$$

212

213 *Equation 2.*

$$k_{off} = \frac{k_u(f)}{\exp \left[ \frac{f - 1/2 k_{eff} \cdot x_t}{f_{\beta}} \right]}$$

214

215 *Equation 3.*

$$\Delta G_{bu} = \frac{(f_{eq})^2}{2k_{eff}}$$

216

217 Here  $\langle f \rangle$  is the most probable rupture force for events at a certain value of loading rate  $r$ ;  $f_{eq}$  is  
 218 the mean force required to irreversibly separate the binding pair (the 'equilibrium force');  $f_{\beta} =$   
 219  $k_B T/x_t$  is the thermal force where  $x_t$  is the distance to the energy barrier,  $k_B$  the Boltzmann

1  
2  
3 220 constant and  $T$  the temperature in Kelvin;  $k_u(f)$  is the unbinding rate at a given force  $f$ ;  $k_{\text{eff}}$  is  
4  
5 221 the effective spring constant,  $k_{\text{eff}}^{-1} = k_{\text{cantilever}}^{-1} + k_{\text{linker}}^{-1}$ . The most probable rupture forces  $\langle f \rangle$   
6  
7 222 were calculated for intervals based on the loading rate  $r$ , with the number of datapoints  $n$  per  
8  
9 223 interval ranging from 10 to 30, so that the maximum error bars on the value of the most  
10  
11 224 probable rupture force  $\langle f \rangle$  in each interval did not exceed 10 pN. DFS (plots of  $\langle f \rangle$  vs.  $\ln(r)$ ) for  
12  
13 225 both sets of experiments were then constructed and the values for the parameters  $f_{\text{eq}}$ ,  $x_t$ ,  $k_{\text{off}}$   
14  
15 226 and  $\Delta G_{\text{bu}}$  were extracted from fits of the F-N-Y model to the DFS for each oligoG. The F-N-  
16  
17 227 Y model has been used recently to determine the length of the minimum sequence of  
18  
19 228 guluronic acids to form a strong, stable calcium-mediated ‘eggbox’ junction<sup>14</sup>.

20 229

21 230 **Results and Discussion**

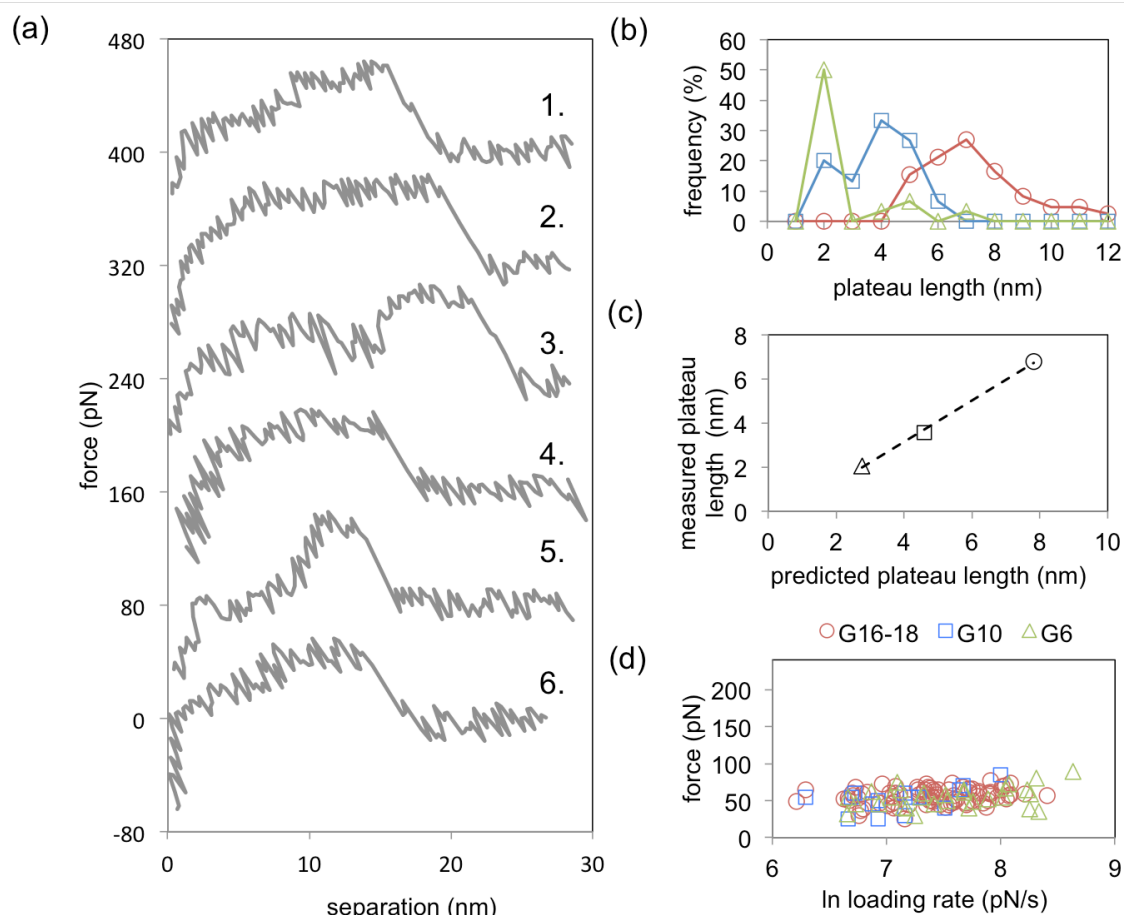
22 231

23  
24  
25 232 In the SCFS experiment, untethered oligoG was allowed to bind in the presence of  $\text{CaCl}_2$  to  
26  
27 233 oligoG tethered to the surface by PEG, as in the conventional SMFS experiment<sup>14</sup>, but with  
28  
29 234 the addition of  $\alpha$ -CD which was threaded over the PEG polymer to form a pseudorotaxane  
30  
31 235 prior to binding the polymer to the surface. A tether on the  $\alpha$ -CD was terminated with an  
32  
33 236 amine group and an AFM probe was functionalised with another PEG spacer, this time  
34  
35 237 terminated with a succinimide group. Previously<sup>23</sup> we have shown that at neutral pH a strong  
36  
37 238 bond was rapidly formed between the amine and succinimide groups, and this bond allowed  
38  
39 239 the AFM probe to manipulate the  $\alpha$ -CD along the polymer chain and over the oligoG.

40 240

41 241 Firstly, in order to confirm that we were observing the pickup and sliding of the CD, we  
42  
43 242 characterised the length of the plateau in force caused by sliding the CD along individual  
44  
45 243 strands of 6-, 10- and 16-18-mer (2-, 4- and 8- $\text{Ca}^{2+}$ ) oligoGs. The force spectra collected do  
46  
47 244 not show the sharp increase in force prior to the terminating rupture point that is typically  
48  
49 245 observed for single molecule stretches in conventional force spectroscopy. Instead, the  
50  
51 246 stretching events start with the force increasing to approximately 40-70 pN, forming a plateau  
52  
53 247 at this force for some distance, before abruptly terminating, with the recorded force returning  
54  
55 248 to zero. Examples of these force spectra are presented in Figure 2a. The length of the plateau  
56  
57 249 region can be determined in the AFM software, and we see the lengths of the three oligomers  
58  
59 250 reflected in the lengths of the plateaus, as presented in Figure 2b. The experimentally  
60  
251 observed plateau lengths are close to the expected lengths of oligoGs of 6, 10 and 16-18  
252 monomers, based on a per monomer length for guluronic acid of 0.435 nm<sup>30</sup> (Figure 2c).

253



254

255 *Figure 2: (a) examples of force curves from the different oligoG experiments: curves 1 and 2*  
 256 *are from the 16-18-mer oligoGs, curves 3 and 4 are from the 10-mer oligoGs and curves 5*  
 257 *and 6 are from the 6-mer oligoGs ; (b) distribution of plateau lengths for the 3 oligomers; (c)*  
 258 *comparison of mean observed length to expected oligomer length for the 3 oligomers; (d)*  
 259 *DFS for sliding CD ring along the 3 oligomers. The scale of the x-axis is the natural*  
 260 *logarithm of the loading rate  $r$  (in pN/s), divided by 1 pN/s.*

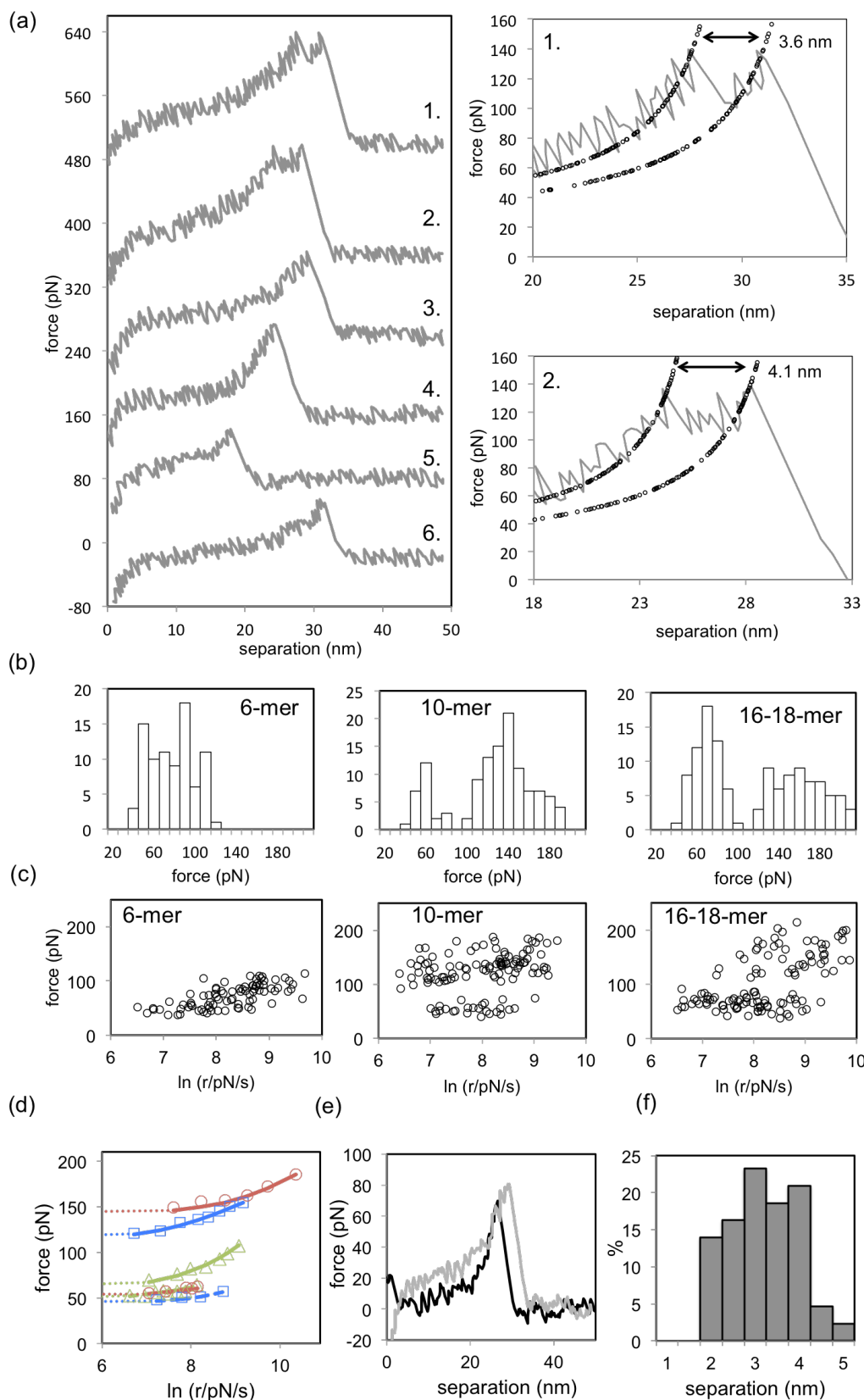
261

262 In order to accurately measure rupture forces when the sliding contact ‘unzips’ the interaction  
 263 between the oligoGs, we must take into account the force required to slide the cyclodextrin  
 264 ring over the oligosaccharide chain. The dynamic force spectrum resulting from a plot of  $f$  vs.  
 265  $\ln(r)$  for these experiments reveals that the three oligomers all show similar behaviour –  
 266 indeed, the DFS for each oligomer can be superimposed on each other and overlap  
 267 extensively, each spectrum showing an almost flat dependence of  $f$  on  $\ln(r)$  (Figure 2d).  
 268 Within the paradigm of the F-N-Y model, a flat dependence of  $f$  on  $\ln(r)$  reflects the  
 269 equilibrium condition, where the rates of unbinding and rebinding (here taken to mean sliding  
 270 on to or off the next monomer in the chain) exceed the rate of loading  $r$  on the bond. This

1  
2  
3 271 means that fits to the F-N-Y model cannot produce reliable values for the kinetic parameters  
4  
5 272  $x_t$  and  $k_{\text{off}}$  but that we can estimate the value of  $f_{\text{eq}}$  (and hence  $\Delta G_{\text{bu}}$ ) for the sliding interaction  
6  
7 273 of the cyclodextrin ring along the polymer strand directly from the most probable plateau  
8  
9 274 force across each spectrum. It is however more difficult to accurately measure the loading  
10  
11 275 rate  $r$  in the transition to these relatively low force plateau events, which impacts on the  
12  
13 276 reliability of the DFS and subsequent fits. Reassurance that the force  $f$  is independent of  $r$   
14  
15 277 comes from the observation that the range of  $f$  observed is relatively narrow, similar to the  
16  
17 278 background thermal noise level of  $\pm 15$  pN, as would be expected when  $f$  is not changing.  
18  
19 279 Thus, applying the F-N-Y model to extract the value of  $f_{\text{eq}}$  produces values of  $43 \pm 11$ ,  $44 \pm 8$   
20  
21 280 and  $54 \pm 12$  pN for the 6-, 10- and 16-18-mer oligoGs respectively, and these values overlap  
22  
23 281 with the mean rupture forces across each dataset. The unbinding energies  $\Delta G_{\text{bu}}$  derived from  
24  
25 282 these values reflect the energy required to thread the cyclodextrin on to, and off, a  
26  
27 283 monosaccharide within the oligoG, a process that occurs for each monomer in the oligomer,  
28  
29 284 producing the observed plateau. Thus, when the values of  $k_{\text{eff}}$  ( $k_{\text{cantilever}} = 14, 13$  and  $25$   
30  
31 285  $\text{pN}\cdot\text{nm}^{-1}$  and  $k_{\text{linker}} = 67 \text{ pN}\cdot\text{m}^{-1}$ )<sup>1</sup> are considered, the energies  $\Delta G_{\text{bu}}$  required to slide the  
32  
33 286 cyclodextrin over individual monomers in the oligoGs are found to be similar to each other,  
34  
35 287 at 47, 50 and 48 kJ/mol for the 6-, 10- and 16-18-mer oligoGs respectively.

36  
37 288  
38  
39 289 Having established the energy required to slide the cyclodextrin ring along the oligomer  
40  
41 290 chain, we can use this approach to unzip specific bonds formed between components of the  
42  
43 291 threaded oligomer and molecules that are introduced into the sample space without tethering  
44  
45 292 to the substrate or AFM probe. Here, the experiment is conducted as just described but  
46  
47 293 untethered oligoGs and calcium ions are injected into the sample space, so that bonds formed  
48  
49 294 between tethered and untethered molecules could be interrogated. The 10-mer oligoG is  
50  
51 295 expected to crosslink a maximum of 4  $\text{Ca}^{2+}$  ions (because the tethered oligoG effectively  
52  
53 296 loses one monomer during conjugation to the PEG<sup>14</sup>), and the 16-18-mer oligoG up to 8  $\text{Ca}^{2+}$   
54  
55 297 ions. When we carry out these experiments, we observe new interactions in addition to the  
56  
57 298 single chain sliding events already characterised. Addition of EDTA effectively abolishes  
58  
59 299 these interactions and we subsequently only observe single chain sliding events, as described  
60  
300 above. Depending on the oligomer under consideration, we observe different behaviour, as  
301  
302 depicted in Figure 3a. In particular we see, in the two shortest oligoGs, some events that more  
303  
304 closely resemble conventional single molecule rupture events, and which have recently been  
described in the alginate system<sup>14</sup>: sharp ruptures at higher forces that return rapidly to zero  
force after the rupture. In contrast, in the 16-18-mer oligoG we observe that once the force

305 reaches similar values to those at which ruptures are observed in the shorter oligomer, there is  
 306 a short region that sometimes resembles two closely following ‘sawtooth’ rupture events



307

308

1  
2  
3 309 *Figure 3. (a) examples of force curves showing the rupture of crosslinks between oligoGs. 1*  
4 *and 2 show ruptures between 16-18-mer oligoGs; 3 and 4 show ruptures between 10-mer*  
5 310 *oligoGs and 5 and 6 show ruptures between 6-mer oligoGs. 1 and 2 are examples of dual*  
6 311 *rupture events: a ‘sawtooth’ double rupture in curve 1 (distance between events = 3.6 nm)*  
7 312 *and a plateau in curve 2 (distance between events = 4.1 nm). (b) histograms of rupture forces*  
8 313 *for (top) 6-mer (middle) 10-mer and (bottom) 16-18-mer oligoGs. (c) dynamic force spectra*  
9 314 *for all data for the three oligomers. . The scale of the x-axis is the natural logarithm of the*  
10 315 *loading rate  $r$  (in pN/s) divided by 1 pN/s. (d) DFS for the three oligomer fractions, split into*  
11 316 *groups according to the force histogram and DFS presented in figure 3b and c. Solid lines*  
12 317 *are fits to the unzipping data for 6-mer ( $\Delta$ ), 10-mer ( $\square$ ) and 16-18-mer ( $\circ$ ) oligoGs, dashed*  
13 318 *lines are fits to the sliding data for the three oligomers and dotted lines are extrapolations to*  
14 319 *the value of  $f_{eq}$  in each case. (e) comparison of force curves from SMFS (black) and SCFS*  
15 320 *(grey) experiments, highlighting the increased force signal originating from the sliding of the*  
16 321 *CD ring along the PEG chain. (f) distribution of distances between first and second rupture*  
17 322 *events in the 16-18-mer oligoG SCFS experiment.*  
18 323  
19 324  
20  
21  
22  
23  
24  
25  
26  
27  
28  
29  
30  
31

32 325 (force curve 1. in figure 3a) and sometimes resembles a plateau (force curve 2. in figure 3a).  
33 326 The existence of these dual events was confirmed by fitting a second freely-jointed chain  
34 327 stretch to the data, and the zoomed spectra in figure 3a show that the data for the two curves  
35 328 are fit by two freely jointed chains each, using the same Kuhn length (0.70 and 0.76 nm) but  
36 329 separated by 3.6 and 4.1 nm respectively. There is a continuum of responses observed  
37 330 following the first rupture in these cases, so distinguishing sawtooth and rupture events is  
38 331 difficult to achieve. As exemplars of this transition, curve 1 is identified as a sawtooth event  
39 332 by the drop in force immediately following the first rupture (33 pN), before the force  
40 333 increases again prior to the second rupture while curve 2 is identified as a plateau event  
41 334 because the force only drops a small amount (16 pN) before reaching a plateau force which is  
42 335 terminated by a brief increase in force. In all cases, these events occur alongside events that  
43 336 resemble those seen in the single chain sliding experiments as presented in Figure 2a. Figure  
44 337 3b shows histograms of the rupture forces and Figure 3c shows plots of force vs  $\ln(r)$  for the  
45 338 three oligomers studied, while the DFS derived from this data is shown in Figure 3d.  
46  
47  
48  
49  
50  
51  
52  
53  
54  
55  
56  
57

58 340 In each case, then, the events fall into two groups, those with sharp rupture events (which  
59 341 may be followed by a plateau or second rupture) and those with only plateaus. In each case  
60 342 the latter group both resembles in form and in force the single chain sliding DFS while the

1  
2  
3 343 former group, at higher forces, constitutes a new type of event well separated from the single  
4  
5 344 chain sliding events. These clusters reflect the types of event discussed above, suggesting that  
6  
7 345 the two types of event can be identified as instances where untethered oligoG bound to the  
8  
9 346 tethered oligoG has been ‘unzipped’ by the action of the cyclodextrin ring sliding along the  
10  
11 347 tethered chain (the ‘unzipping’ group), and instances where no untethered oligoG has bound  
12  
13 348 to the tethered chain and the cyclodextrin slide freely along and off, as it does in the absence  
14  
15 349 of untethered oligoG (the ‘sliding’ group). By comparing the numbers of the two types of  
16  
17 350 event we can estimate the extent of binding of the untethered oligoG to the tethered oligoG,  
18  
19 351 and in these cases we observe unzipping in 81, 76 and 52% of observed events for the 6-, 10-  
20  
21 352 and 16-18-mer oligoGs respectively. The existence of the sliding group of events reveals that  
22  
23 353 binding between the oligoGs is not 100% efficient, even when minutes are allowed for  
24  
25 354 binding to occur. In the 6-mer oligoG the forces measured in the unzipping group are  
26  
27 355 significantly lower than those in the unzipping groups for the two longer oligoGs. This  
28  
29 356 distribution of forces for the three oligomers bears out the conclusion of our previous work<sup>14</sup>,  
30  
31 357 where we showed (at long interaction times) that  $\text{Ca}^{2+}$ -mediated crosslinks between short  
32  
33 358 oligoGs ruptured at lower forces than those between oligoGs of 10 monomers or more.

34  
35 360 The DFS for the unzipping groups each show evidence that the data encompass the transition  
36  
37 361 between the equilibrium and non-equilibrium states and can be fit by the F-N-Y model,  
38  
39 362 allowing the estimation of the parameters  $x_t$ ,  $k_{\text{off}}$  and  $f_{\text{eq}}$  (and hence  $\Delta G_{\text{bu}}$ ). This finding is, on  
40  
41 363 first consideration, surprising: we have established that this is a slowly forming bond so we  
42  
43 364 do not expect to find a fast rebinding rate during its rupture. It has been proposed<sup>31</sup> that the  
44  
45 365 slow binding kinetics of elastic polyelectrolyte crosslinks such as the eggbox junction arise  
46  
47 366 from the time taken for the polymeric strands to align and form the initial crosslinks in  
48  
49 367 coordination with the  $\text{Ca}^{2+}$  ions. In the situation arising during the sliding of the CD ring  
50  
51 368 along the oligoG chain and the consequent rupture of the crosslink, all components of the  
52  
53 369 crosslink remain close together so rebinding may occur rapidly. The rate-limiting step in  
54  
55 370 bond formation is then the initial rearrangement of the polyelectrolyte chains, which is not  
56  
57 371 significantly perturbed in the time it takes for the CD ring to move forward: indeed, the size  
58  
59 372 and stiffness of the polymer chains that limit the bond formation rate in the first instance may  
60  
373 also be the factors driving rapid rebinding immediately following unbinding. Conversely, the  
374 sliding groups show little dependence of  $f$  on  $r$ , so only  $f_{\text{eq}}$  (and  $\Delta G_{\text{bu}}$ ) may be measured.  
375

376 To accurately characterise the rupture we must deconvolute the force required simply to slide  
 377 the cyclodextrin along the tethered oligoG from the force required to unzip the bound  
 378 untethered oligoG. Since both processes occur simultaneously the overall force observed  
 379 consists of the sum of these two forces, so the value of  $f_{eq}$  for the unzipping process is  
 380 obtained by subtracting the value of  $f_{eq}$  for the single chain sliding event from the overall  $f_{eq}$   
 381 observed for the interaction at low loading rates and derived from the DFS shown in Figure  
 382 3d. The resulting force we call the excess  $f_{eq}$ , and the free energy calculated from it is the  
 383 excess  $\Delta G_{bu}$ .

384  
 385 *Table 1. Values of parameters from fits of the data for the sliding and unzipping events for*  
 386 *the three oligomers to the F-N-Y model. Values are given as mean  $\pm$  SD.*

OligoG interaction	$f_{eq}$ (pN)	Excess $f_{eq}$ (pN)	Excess $\Delta G_{bu}$ (kJ/mol)	$x_t$ (nm)	$k_{off}$ ( $s^{-1}$ )
6 sliding	44 $\pm$ 6	n.d.	n.d.	n.d.	n.d.
6 unzipping	58 $\pm$ 12	20 $\pm$ 12	10.3 $\pm$ 6.1	0.08 $\pm$ 0.03	21.3 $\pm$ 12.6
10 sliding	43 $\pm$ 7	n.d.	n.d.	n.d.	n.d.
10 unzipping	112 $\pm$ 23	68 $\pm$ 24	125 $\pm$ 30	0.12 $\pm$ 0.05	2.1 $\pm$ 1.8
16 sliding	51 $\pm$ 9	n.d.	n.d.	n.d.	n.d.
16 unzipping	141 $\pm$ 31	87 $\pm$ 26	125 $\pm$ 33	0.10 $\pm$ 0.04	7.2 $\pm$ 6.1

387  
 388 Table 1 presents the values of the derived parameters. Of particular note in this data is the  
 389 fact that the values of excess  $\Delta G_{bu}$  for the 10-mer and the 16-18-mer are similar, at 125  
 390 kJ/mol. Assuming, for the 10-mer oligoG interaction, 4  $Ca^{2+}$  ions are involved, this value  
 391 corresponds to 31 kJ/mol per  $Ca^{2+}$  ion, in close agreement with the value measured using  
 392 conventional SMFS at long dwell times (36 kJ/mol/  $Ca^{2+}$ )<sup>13</sup> and falling within the range of  
 393 values measured<sup>32</sup> or calculated from simulations<sup>33,34</sup> (25-60 kJ/mol/  $Ca^{2+}$ ). The calculated  
 394 values for excess  $\Delta G_{bu}$  for the 10-mer and the 16-18-mer are similar even though the values  
 395 of excess  $f_{eq}$  differ, because accurate calculation of the free energy of unbinding requires the  
 396 effective spring constant of the cantilever and polymer tethers<sup>1,3</sup>, and in the case of the  
 397 experiments conducted here the cantilever spring constants for the 10-mer and 16-18-mer  
 398 experiments were 13 and 25 pN/nm respectively. The excess  $\Delta G_{bu}$  for the 6-mer is much  
 399 smaller at 10 kJ/mol, similar to the value obtained from conventional SMFS<sup>14</sup>. Values for the  
 400 kinetic off-rate,  $k_{off}$ , for the two longest oligomers are also similar to each other (2.1 $\pm$ 1.8 and  
 401 7.2 $\pm$ 6.1  $s^{-1}$  for the 10-mer and the 16-18-mer respectively) but much higher (21.3  $s^{-1}$ ) for the

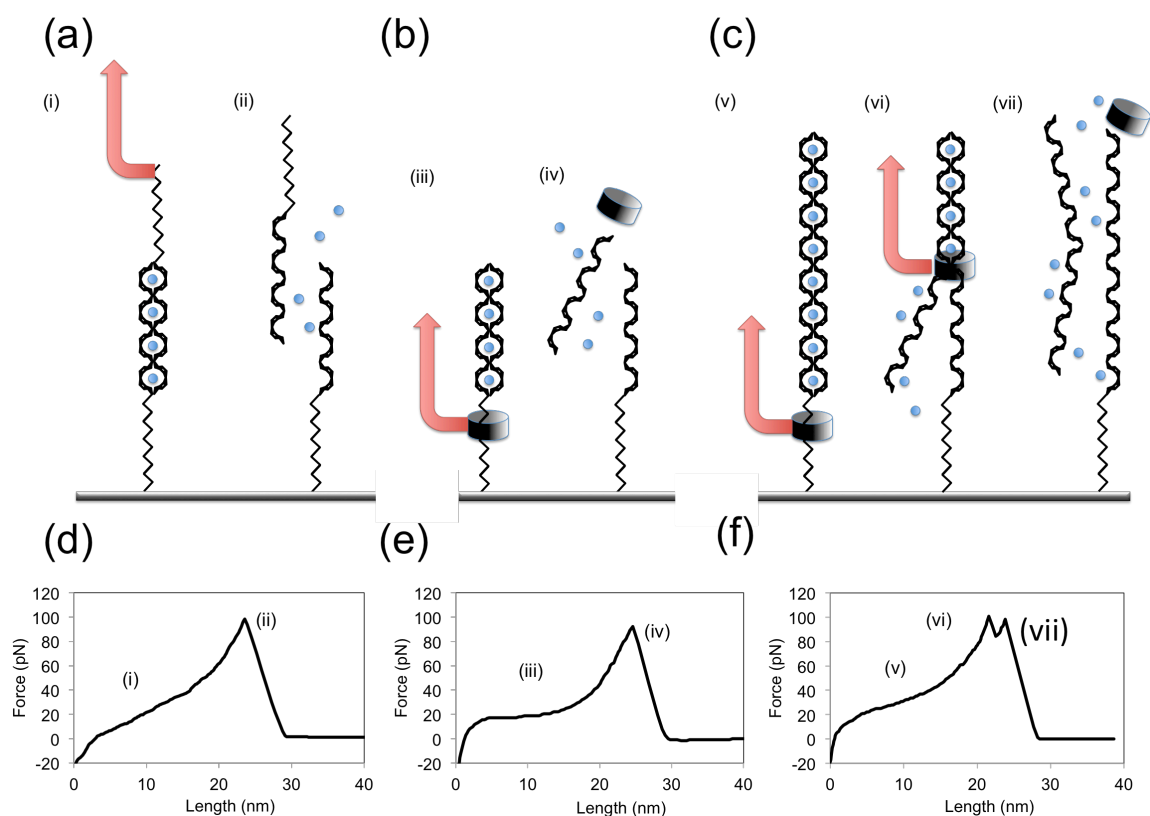
1  
2  
3 402 6-mer. Values of  $x_t$  for the three oligomers are similar to each other, at about 1 Ångström, a  
4  
5 403 value that reflects the distance the crosslink must be distorted before it ruptures. A key  
6  
7 404 observation is that the range of forces observed is narrower for the sliding contact experiment  
8  
9 405 than was recorded in the conventional SMFS experiment<sup>14</sup>: in the previous SMFS work,  $f$   
10  
11 406 ranged from 50-70 pN up to 250 and 450 pN for the 10-mer and 16-18-mers over 3 decades  
12  
13 407 of loading rate, whereas in the present study the range of forces differs by less than 100 pN  
14  
15 408 over a similar range of loading rates (Figures 3b-d). This observation suggests that at the  
16  
17 409 range of loading rates achieved in this experiment the bond remained close to the equilibrium  
18  
19 410 regime where rapid rebinding is possible, only being taken away from this regime at the  
20  
21 411 highest loading rates. This reflects the processive nature of the rupture event in the sliding  
22  
23 412 contact experiment. Instead of tension being applied along the whole crosslink, as it is when  
24  
25 413 the oligomers are pulled apart in conventional SMFS, in the sliding contact experiment the  
26  
27 414 crosslink is addressed one monomer at a time. Thus, for both the 10-mer and the 16-18-mer,  
28  
29 415 the initial unzipping event was identical and reflects the same initial opening up of the  
30  
31 416 crosslink, which is much stronger than the opening of the crosslink between 6-mer oligoGs.  
32  
33 417 Further evidence that the group of force curves we have identified as unzipping events reflect  
34  
35 418 the interaction of the CD ring with the oligoG crosslink comes from a comparison with force  
36  
37 419 curves obtained in the conventional oligomer separation SMFS experiment<sup>14</sup>, as depicted in  
38  
39 420 Figure 3e. Here, at positions prior to the increase in force that precedes crosslink rupture, we  
40  
41 421 observe that the force recorded in the SCFS experiment is higher and more plateau-like than  
42  
43 422 the corresponding SMFS experiment. This is due to the sliding of the CD ring along the PEG  
44  
45 423 chain, a feature previously observed in other SCFS experiments<sup>23</sup>.

424

44 425 We can therefore conclude that the state or number of crosslinked monomers downstream of  
45  
46 426 the first influences the force required to rupture the crosslink, just as it does in conventional  
47  
48 427 SMFS, despite the different way in which the tension is applied to the junction. Thus the  
49  
50 428 junction is not unzipped one monomer at a time, but the first monomer is stabilised in the  
51  
52 429 crosslink by its downstream neighbours, so that the 4 Ca<sup>2+</sup> crosslink fails as a single unit  
53  
54 430 (again, as it does in conventional SMFS). In the case of the 10-mer, the initial opening of the  
55  
56 431 junction is sufficient to destabilise the rest of the junction so a sharp rupture is observed. This  
57  
58 432 reflects the fact that the minimum strong crosslink requires 4 Ca<sup>2+</sup> ions, and that crosslinks  
59  
60 433 involving fewer Ca<sup>2+</sup> ions fail at lower forces. In the 16-18-mer oligoG the junction is long  
434  
435 434 enough that the opening of the initial 4 Ca<sup>2+</sup> crosslink does not destabilise the entire junction,  
435 since more than 4 Ca<sup>2+</sup> ions remain in the crosslink, so a second rupture event (or a plateau in

1  
2  
3 436 force) is observed as the cyclodextrin ring slides along the chain, unzipping interactions until  
4  
5 437 destabilisation occurs. Plateaus, rather than a ‘sawtooth’ profile, would be expected to be  
6  
7 438 observed when the CD ring encounters the next crosslinked sequence before the polymer  
8  
9 439 chain has had time to relax and release the tension on the CD, or when the freed end of the  
10  
11 440 oligoG remains to obstruct the CD as it passes along the tethered chain, whereas sawtooth  
12  
13 441 profiles of double ruptures would be expected to be observed in cases where the freed chain  
14  
15 442 happens to move away from the sliding CD. Figure 3a shows examples of sawtooth and  
16  
17 443 rupture events. Figure 3f shows the distribution of the distances between the first and  
18  
19 444 subsequent rupture events (and the lengths of plateaus) following initial rupture in the 16-18-  
20  
21 445 mer, which has a peak at 3-4 nm. This value is close to the difference in length between the  
22  
23 446 10-mer and 16-18-mer oligoGs presented in Figures 2b and c (3.9 nm for the 10-mer and 7.0  
24  
25 447 nm for the 16-18-mer) and so reflects a situation in which, after disrupting 8 or so monomers  
26  
27 448 taking part in the initial crosslink, the CD ring must slide along the polymer chain to address  
28  
29 449 the remaining interacting monomers. This model thus requires cooperativity across several  
30  
31 450 monomers. Voulgarakis et al<sup>22</sup> considered the applicability of a sliding contact force  
32  
33 451 spectroscopy technique such as the one realised here as a method for sequencing DNA, using  
34  
35 452 the CD ring to rupture the interactions between basepairs with the different forces required to  
36  
37 453 rupture A-T and G-C interactions used as the basis for reconstructing the sequence. In this  
38  
39 454 work they simulated the sliding contact experiment and found that the basepair interactions  
40  
41 455 tended to rupture in bursts rather than individually, and that the force required to rupture an  
42  
43 456 individual basepair depended on the identity of the next 5 or so basepairs in the sequence.  
44  
45 457 Thus we can expect the number of consecutive Ca<sup>2+</sup> mediated interacting monomers in the  
46  
47 458 eggbox junction to determine the force required to unzip it, while the much lower temporal  
48  
49 459 resolution of the AFM experiment in comparison to the simulation means that we would  
50  
51 460 observe such rapid bursts of rupture events as a single event. Figure 4 illustrates the proposed  
52  
53 461 progress of the rupture events in conventional SMFS and SCFS, highlighting the different  
54  
55 462 ways in which the crosslink is addressed and ruptured. Finally it may be noted that rotaxanes  
56  
57 463 formed between CD beads and PEG axes can accommodate multiple beads on a single axis<sup>18</sup>.  
58  
59 464 This is likely to occur in the SCFS experiment too and may result in the AFM probe dragging  
60  
465 a ‘train’ of CD beads along the oligomer. The first bead in the train will induce the rupture of  
466 any eggbox junctions and the rest of the beads will then slide along and off the chain,  
467 potentially yielding subtle differences in the resulting force curves that we have not been able  
468 to differentiate from the single bead case.

469



470

471 *Figure 4. sketches of the arrangements of oligomers,  $\text{Ca}^{2+}$  ions and CD rings during (a)*  
 472 *SMFS of 10-mer oligoG, (b) SCFS of 10-mer oligoG and (c) SCFS of 16-18-mer oligoG.*  
 473 *Arrows depict the point of contact of the force transducer and the direction in which force is*  
 474 *applied in each case. (d-f) force curves corresponding to (a-c) above, with the steps (i) – (vii)*  
 475 *highlighted in each case.*

476

## 477 Conclusions

478

479 Single molecule force spectroscopy remains a powerful tool for measuring the strength of  
 480 individual bonds between molecules brought together transiently. The timescale of the SMFS  
 481 experiment is expected to be sufficient for many interactions between small molecules to  
 482 reach equilibrium during the time that the two molecules are close enough to each other to  
 483 interact. However, particularly in the case of crosslinking interactions between polymers,  
 484 times in excess of 1 second may be required for the crosslink to reach its fully equilibrated  
 485 state. Here we have shown, using the example of the  $\text{Ca}^{2+}$ -mediated crosslink between  
 486 oligomers of guluronic acid, that an alternative iteration of single molecule force  
 487 spectroscopy may be used to accurately measure the free energy of unbinding of slowly  
 488 forming bonds after they have reached equilibrium. We explore the mechanics of the rupture

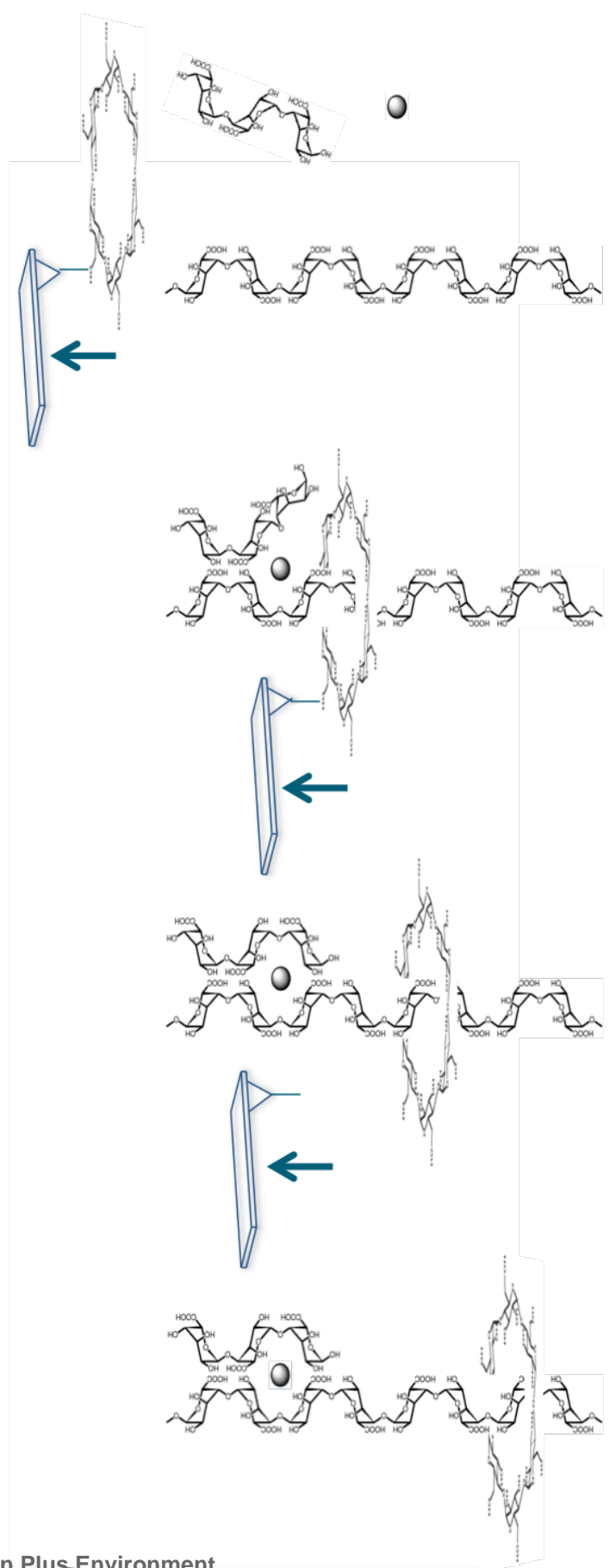
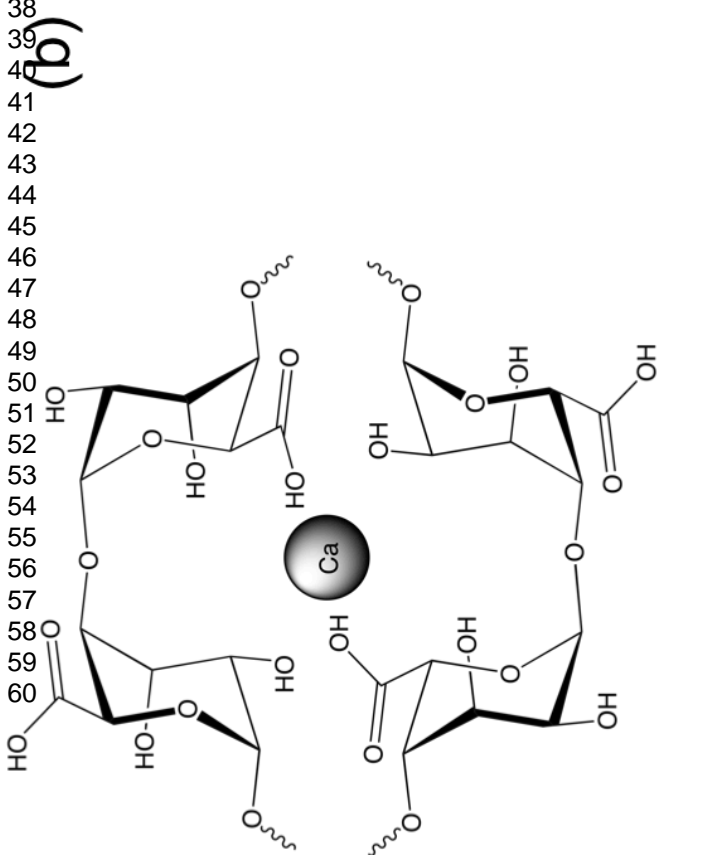
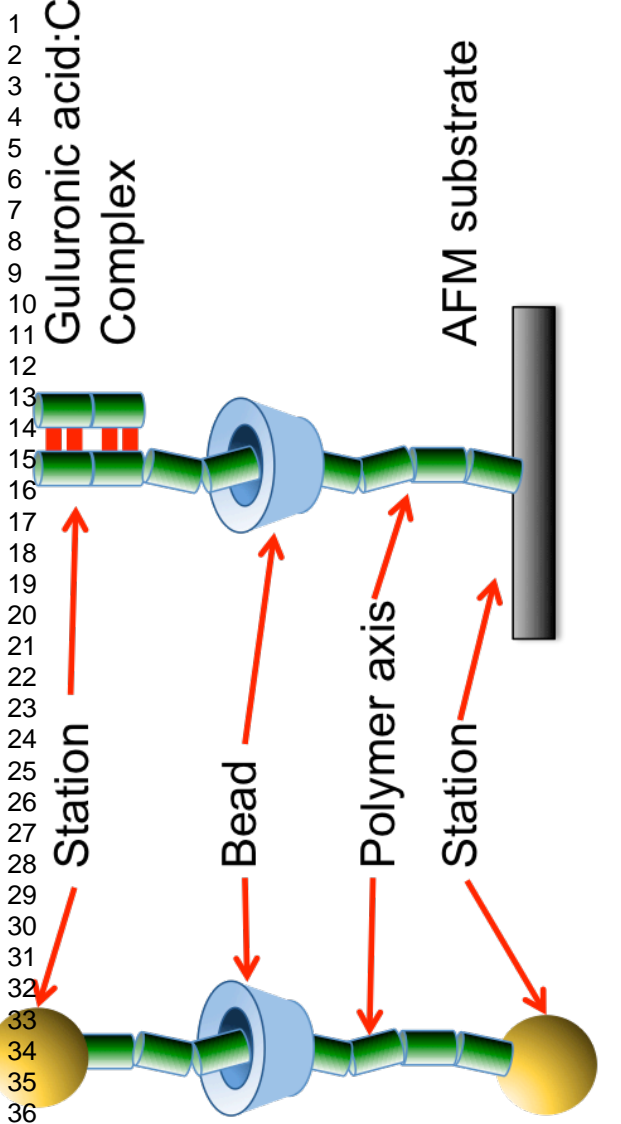
1  
2  
3 489 event caused by unzipping the crosslink with the CD ring and show that we are able to  
4  
5 490 achieve the predicted advantages that this approach holds over conventional SMFS, namely  
6  
7 491 the lack of tethering of the binding partner to the AFM probe and control over the direction in  
8  
9 492 which the bond is attacked. The results allow us to set a value for the free energy required to  
10  
11 493 rupture the minimum  $\text{Ca}^{2+}$ -mediated crosslink between oligoguluronic acid chains, an  
12  
13 494 interaction that governs the properties of the important polysaccharide alginate, of 125  
14  
15 495 kJ/mol.  
16  
17 496

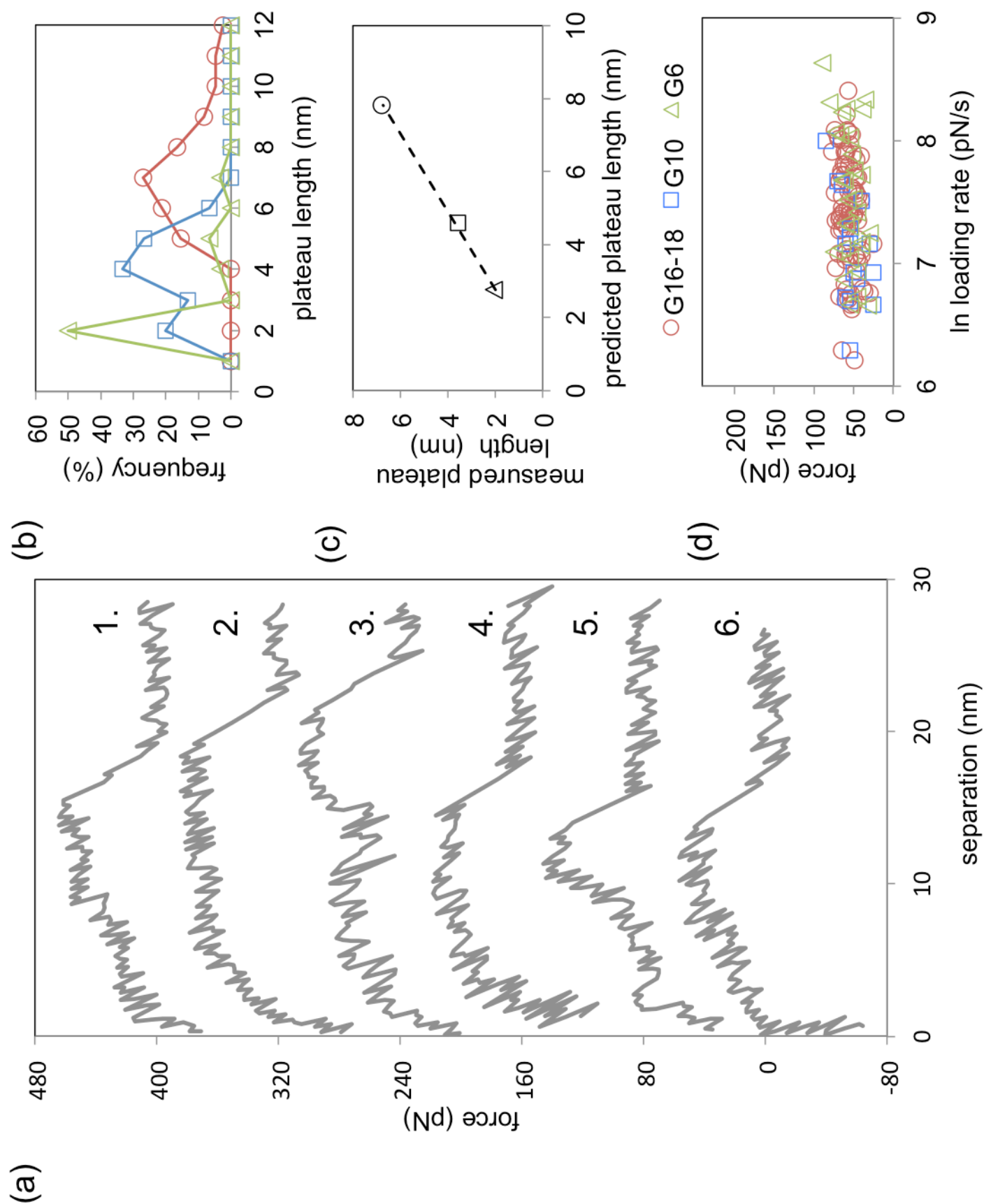
## 17 497 **References**

- 18  
19 498  
20  
21 499 (1) Noy, A.; Friddle, R. W. Practical single molecule force spectroscopy: how to  
22  
23 500 determine fundamental thermodynamic parameters of intermolecular bonds with an atomic  
24  
25 501 force microscope. *Methods* **2013**, *60* (2), 142–150.  
26  
27 502 (2) Evans, E. Probing the relation between force - Lifetime - and chemistry in single  
28  
29 503 molecular bonds. *Annu Rev Bioph Biom* **2001**, *30*, 105–128.  
30  
31 504 (3) Friddle, R. W.; Noy, A.; De Yoreo, J. J. Interpreting the widespread nonlinear force  
32  
33 505 spectra of intermolecular bonds. *Proceedings of the National Academy of Sciences* **2012**, *109*  
34  
35 506 (34), 13573–13578.  
36  
37 507 (4) Coppari, E.; Santini, S.; Bizzarri, A. R.; Cannistraro, S. Kinetics and binding  
38  
39 508 geometries of the complex between  $\beta$ 2-microglobulin and its antibody: An AFM and SPR  
40  
41 509 study. *Biophys. Chem.* **2016**, *211*, 19–27.  
42  
43 510 (5) Gilbert, Y.; Deghorain, M.; Wang, L.; Xu, B.; Pollheimer, P. D.; Gruber, H. J.;  
44  
45 511 Errington, J.; Hallet, B.; Haulot, X.; Verbelen, C.; Hols, P.; Dufrene, Y. F. Single-Molecule  
46  
47 512 Force Spectroscopy and Imaging of the Vancomycin/ d-Ala- d-Ala Interaction. *Nano Lett*  
48  
49 513 **2007**, *7* (3), 796–801.  
50  
51 514 (6) Rao, J.; Lahiri, J.; Isaacs, L.; Weis, R. M.; Whitesides, G. M. A Trivalent System  
52  
53 515 from Vancomycin·d-Ala-d-Ala with Higher Affinity Than Avidin·Biotin. *Science* **1998**, *280*  
54  
55 516 (5364), 708–711.  
56  
57 517 (7) Jianghong Rao; Joydeep Lahiri; Robert M Weis, A.; Whitesides, G. M. Design,  
58  
59 518 Synthesis, and Characterization of a High-Affinity Trivalent System Derived from  
60  
519 Vancomycin and l-Lys-d-Ala-d-Ala; *J. Am. Chem. Soc.*, 2000; Vol. 122, pp 2698–2710.  
520  
521 (8) Rao, J.; Whitesides, G. M. Tight Binding of a Dimeric Derivative of Vancomycin  
with Dimeric l-Lys-d-Ala-d-Ala; *J. Am. Chem. Soc.*, 1997; Vol. 119, pp 10286–10290.

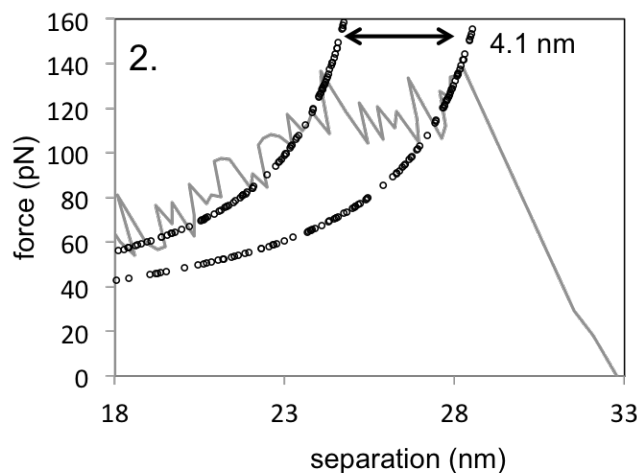
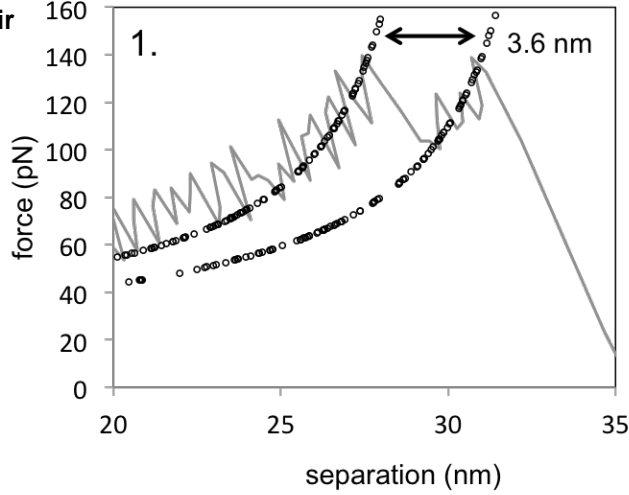
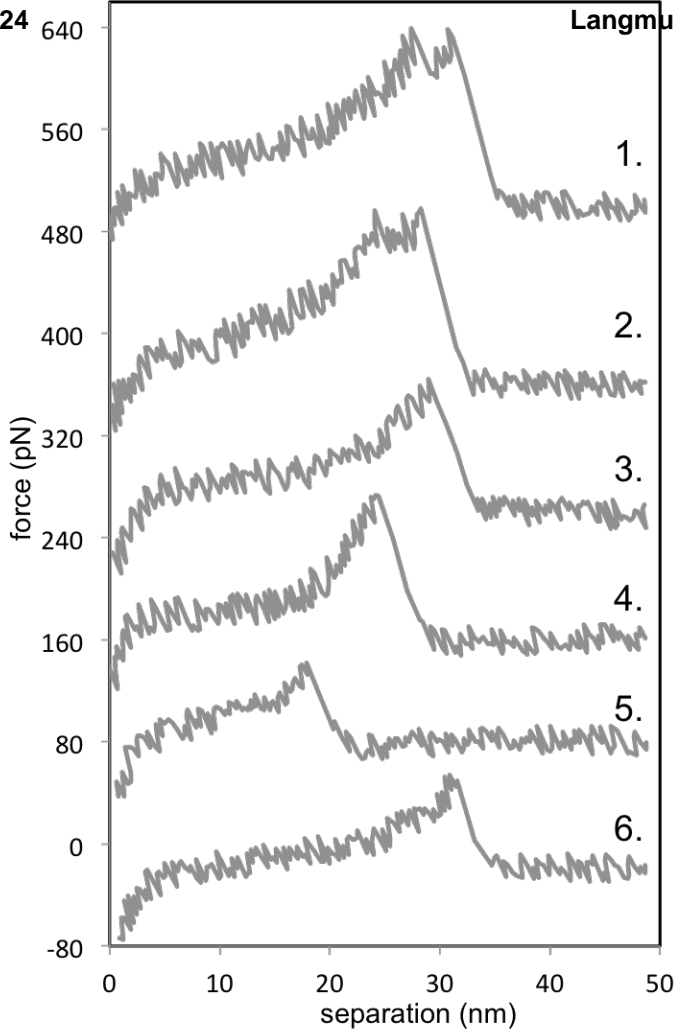
- 1  
2  
3 522 (9) Sundram, U. N.; Griffin, J. H.; Nicas, T. I. Novel vancomycin dimers with activity  
4 523 against vancomycin-resistant enterococci. *J. Am. Chem. Soc.*, **1996**, *118*, 13107-13108
- 5  
6 524 (10) Hulme, E. C.; Trevethick, M. A. Ligand binding assays at equilibrium: validation and  
7 525 interpretation. *Br J Pharmacol* **2010**, *161* (6), 1219–1237.
- 8  
9 526 (11) Larobina, D., & Cipelletti, L. (2013). Hierarchical cross-linking in physical alginate  
10 527 gels: a rheological and dynamic light scattering investigation. *Soft Matter*, **2013**, *9*, 10005–  
11 528 10015.
- 12  
13 529 (12) Secchi, E., Roversi, T., Buzzaccaro, S., Piazza, L., & Piazza, R. Biopolymer gels with  
14 530 physical cross-links: gelation kinetics, aging, heterogeneous dynamics, and macroscopic  
15 531 mechanical properties. *Soft Matter* **2013**, *9*, 3931–3944.
- 16  
17 532 (13) Siviello, C., Greco, F., & Larobina, D. Analysis of linear viscoelastic behaviour of  
18 533 alginate gels: effects of inner relaxation, water diffusion, and syneresis. *Soft Matter* **2015**, *11*,  
19 534 6045–6054.
- 20  
21 535 (14) Bowman, K. A.; Aarstad, O. A.; Nakamura, M.; Stokke, B. T.; Skjåk-Braek, G.;  
22 536 Round, A. N. Single molecule investigation of the onset and minimum size of the calcium-  
23 537 mediated junction zone in alginate. *Carbohydr Polym* **2016**, *148*, 52–60.
- 24  
25 538 (15) Ma, C. D.; Acevedo-Vélez, C.; Wang, C.; Gellman, S. H.; Abbott, N. L. Interaction of  
26 539 the Hydrophobic Tip of an Atomic Force Microscope with Oligopeptides Immobilized Using  
27 540 Short and Long Tethers *Langmuir* **2016**, *32* (12), 2985–2995.
- 28  
29 541 (16) Guo, S., Li, N., Lad, N., Desai, S., & Akhremitchev, B. B. Distributions of parameters  
30 542 and features of multiple bond ruptures in force spectroscopy by atomic force microscopy.  
31 543 *The Journal of Physical Chemistry C* **2010**, *114*, 8755–8765.
- 32  
33 544 (17) Harada A.; Kamachi, M. *Macromolecules*, **1990**, *23*, 2821.
- 34  
35 545 (18) Wenz, G.; Han, B. H.; Muller, A. *Chem. Rev.*, **2006**, *106*, 782.
- 36  
37 546 (19) Shigekawa, H.; Miyake, K.; Sumaoka, J.; Harada, A.; Komiyama, M. *J Am Chem*  
38 547 *Soc*, **2000**, *122*, 5411.
- 39  
40 548 (20) Brough, B.; Northrop, B. H.; Schmidt, J. J.; Tseng, H.-R.; Houk, K. N.; Stoddart, J.  
41 549 F.; Ho, C.-M. *P Natl Acad Sci USA*, **2006**, *103*, 8583.
- 42  
43 550 (21) Lussis, P.; Svaldo-Lanero, T.; Bertocco, A.; Fustin, C.-A.; Leigh, D. A.; Duwez, A.-S.  
44 551 A single synthetic small molecule that generates force against a load. *Nature Nanotechnology*  
45 552 **2011**, *6* (9), 553–557.
- 46  
47 553 (22) Voulgarakis, N. K.; Redondo, A.; Bishop, A. R.; Rasmussen, K. O. Sequencing DNA by  
48 554 dynamic force spectroscopy: limitations and prospects. *Nano Lett.* **2006**, *6*, 1483-1486.

- 1  
2  
3 555 (23) Dunlop, A.; Wattoo, J.; Hasan, E. A.; Cosgrove, T.; Round, A. N. Mapping the  
4 556 positions of beads on a string: dethreading rotaxanes by molecular force spectroscopy.  
5 557 *Nanotechnology* **2008**, *19* (34), 345706.  
6  
7 558 (24) Ashcroft, B. A.; Spadola, Q.; Qamar, S.; Zhang, P.; Kada, G.; Bension, R.; Lindsay,  
8 559 S. M. *Small*, **2008**, *4*, 1468.  
9  
10 560 (25) Qamar, S.; Williams, P. M.; Lindsay, S. M. *Biophys. J.* **2008**, *94*, 1233.  
11  
12 561 (26) Gray, G. Antibodies to carbohydrates: preparation of antigens by coupling  
13 562 carbohydrates to proteins by reductive amination with cyanoborohydride. *Methods in*  
14 563 *Enzymology* **1978**, *50*, 155–160.  
15  
16 564 (27) Takemasa, M., Sletmoen, M., & Stokke, B. T. Single molecular pair interactions  
17 565 between hydrophobically modified hydroxyethyl cellulose and amylose determined by  
18 566 dynamic force spectroscopy. *Langmuir* **2009**, *25*, 10174–10182.  
19  
20 567 (28) Gunning, A. P., Bongaerts, R. J. M., & Morris, V. J. Recognition of galactan  
21 568 components of pectin by galectin-3. *The FASEB Journal* **2009**, *23*, 415–424.  
22  
23 569 (29) Hutter, J. L.; Bechhoefer, J. Calibration of atomic-force microscope tips *Rev Sci*  
24 570 *Instrum* **1993**, *64* (7), 1868–1873.  
25  
26 571 (30) Atkins, E. D., Nieduszynski, I. A., Mackie, W., Parker, K. D., & Smolko, E. E.  
27 572 Structural components of alginic acid. II. The crystalline structure of poly-alpha-l-guluronic  
28 573 acid. Results of X-ray diffraction and polarized infrared studies. *Biopolymers* **1973**, *12*,  
29 574 1879–1887.  
30  
31 575 (31) Borukhov, I.; Bruinsma, R. F.; Gelbart, W. M.; Liu, A. J. Elastically driven linker  
32 576 aggregation between two semiflexible polyelectrolytes. *Phys Rev Lett* **2001**, *86* (10), 2182–  
33 577 2185.  
34  
35 578 (32) Fang, Y., Al-Assaf, S., Phillips, G. O., Nishinari, K., Funami, T., Williams, P. A., et  
36 579 al. Multiple steps and critical behaviors of the binding of calcium to  
37 580 alginate. *Journal of Physical Chemistry B* **2007**, *111*, 2456–2462.  
38  
39 581 (33) Braccini, I., & Perez, S. Molecular basis of Ca(2+)-induced gelation in alginates and  
40 582 pectins: the egg-box model revisited. *Biomacromolecules* **2001**, *2*, 1089–1096.  
41  
42 583 (34) Plazinski, W. Molecular basis of calcium binding by polyguluronate chains: revising  
43 584 the egg-Box model. *Journal of Computational Chemistry* **2011**, *32*, 2988–2995.  
44  
45 585  
46  
47  
48  
49  
50  
51  
52  
53  
54  
55  
56  
57  
58  
59  
60

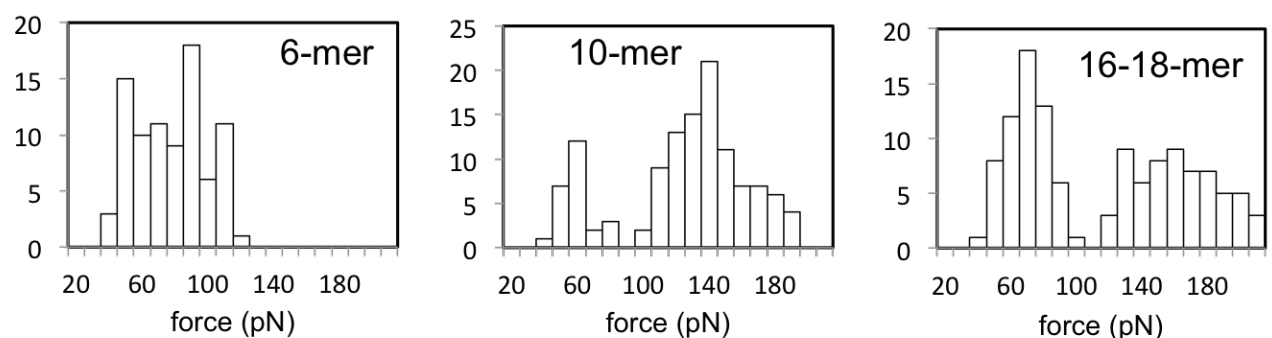




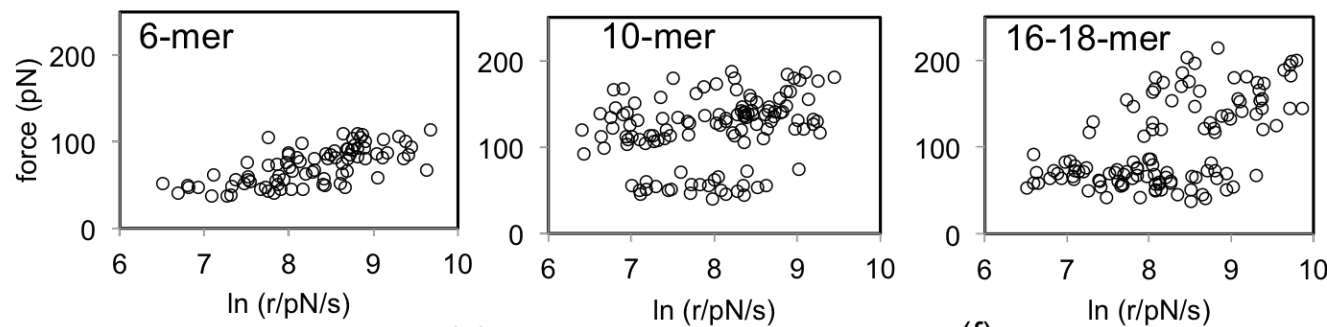
1  
2  
3  
4  
5  
6  
7  
8  
9  
10  
11  
12  
13  
14  
15  
16  
17  
18  
19  
20  
21  
22  
23  
24  
25  
26  
27  
28  
29  
30  
31  
32  
33  
34  
35  
36  
37  
38  
39  
40  
41  
42  
43  
44  
45  
46  
47  
48  
49  
50  
51  
52  
53  
54  
55  
56  
57  
58  
59  
60



(b)



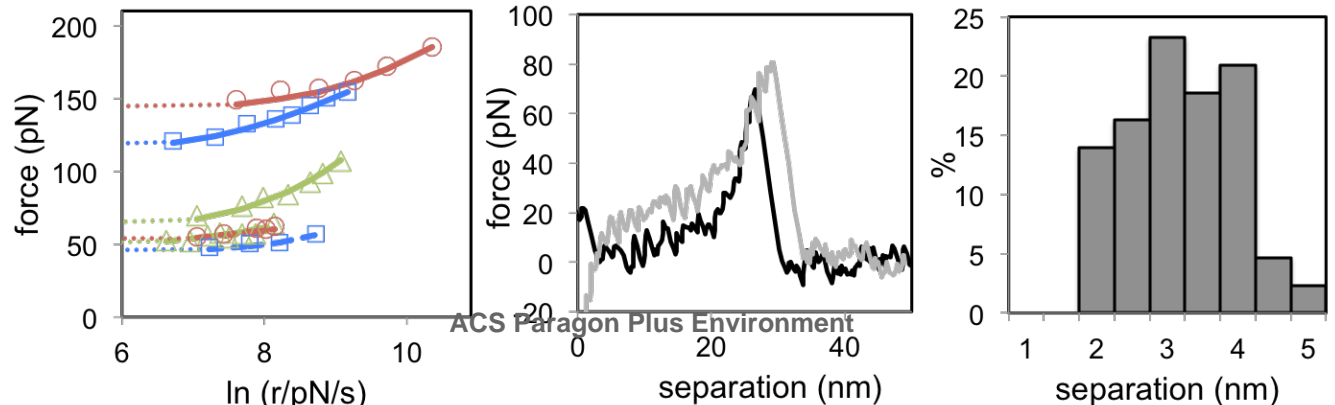
(c)



(d)

(e)

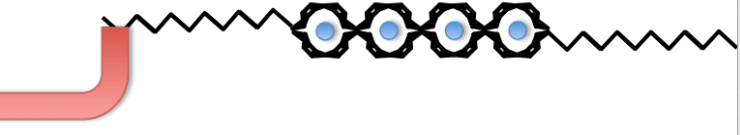
(f)



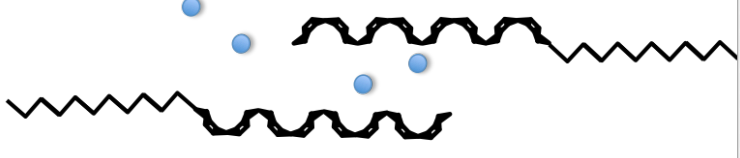
1  
2  
3  
4  
5  
6  
7  
8  
9  
10  
11  
12  
13  
14  
15  
16  
17  
18  
19  
20  
21  
22  
23  
24  
25  
26  
27  
28  
29  
30  
31  
32  
33  
34  
35  
36  
37  
38  
39  
40  
41  
42  
43  
44  
45  
46  
47  
48  
49  
50  
51  
52  
53  
54  
55  
56  
57  
58  
59  
60

(a)

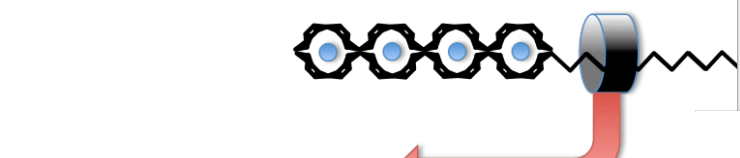
(i)



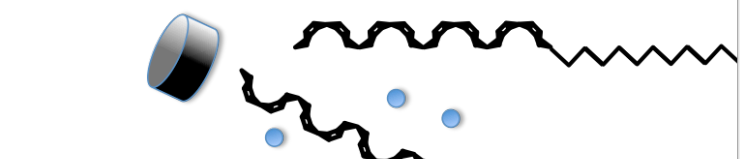
(ii)



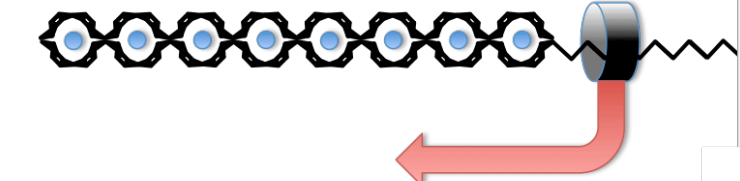
(iii)



(iv)



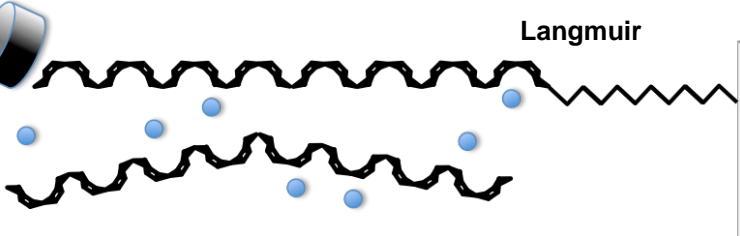
(v)



(vi)

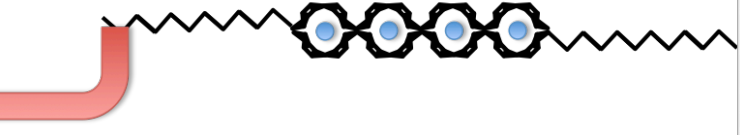


(vii)

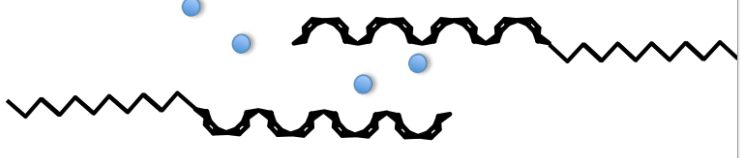


(b)

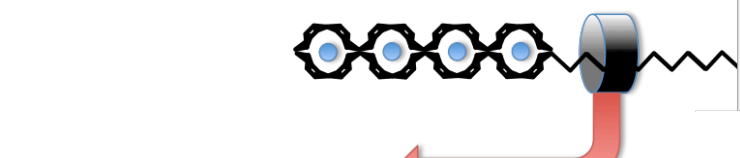
(i)



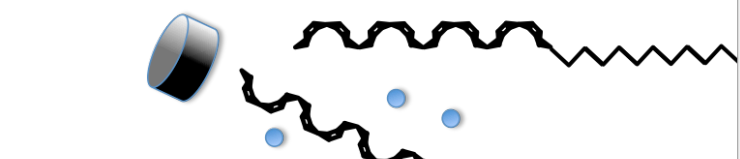
(ii)



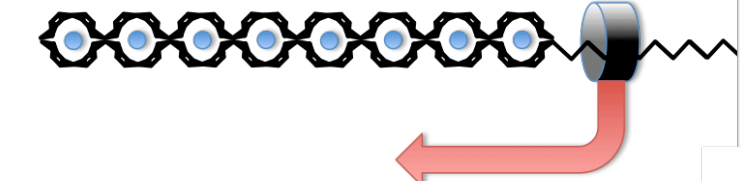
(iii)



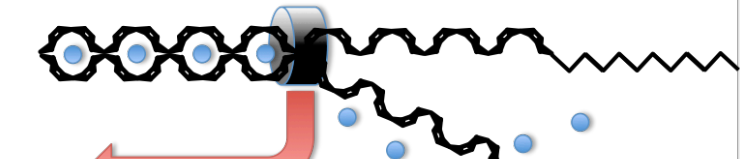
(iv)



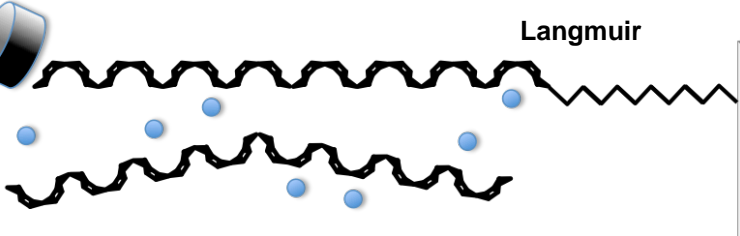
(v)



(vi)

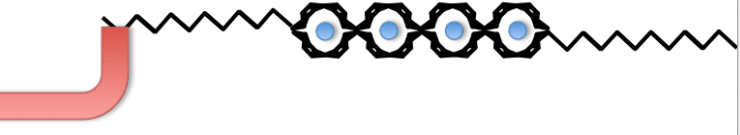


(vii)

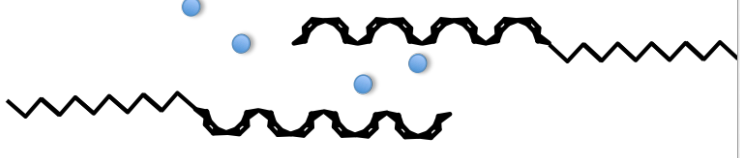


(c)

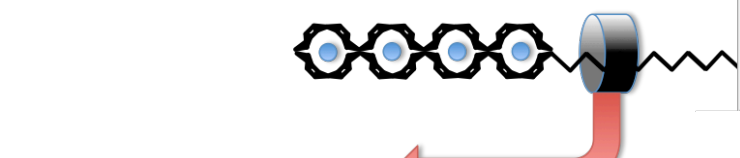
(i)



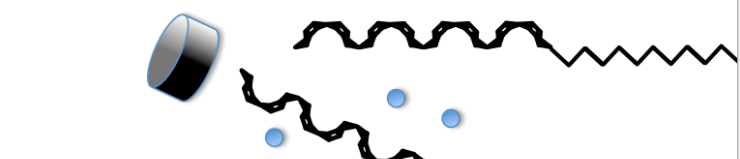
(ii)



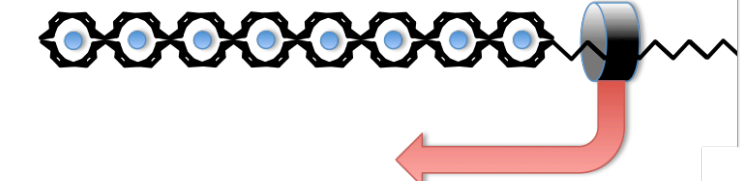
(iii)



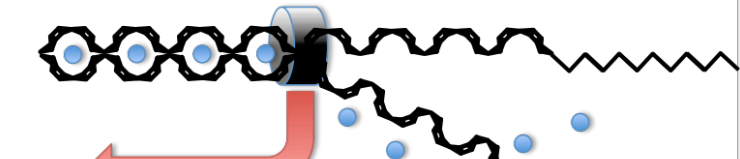
(iv)



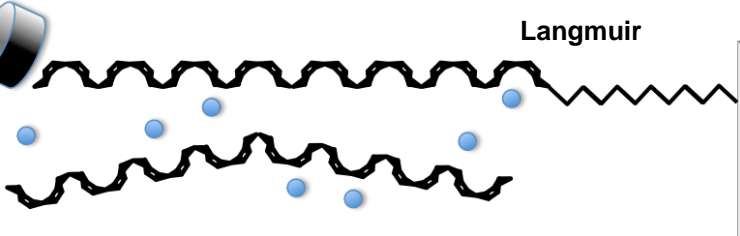
(v)



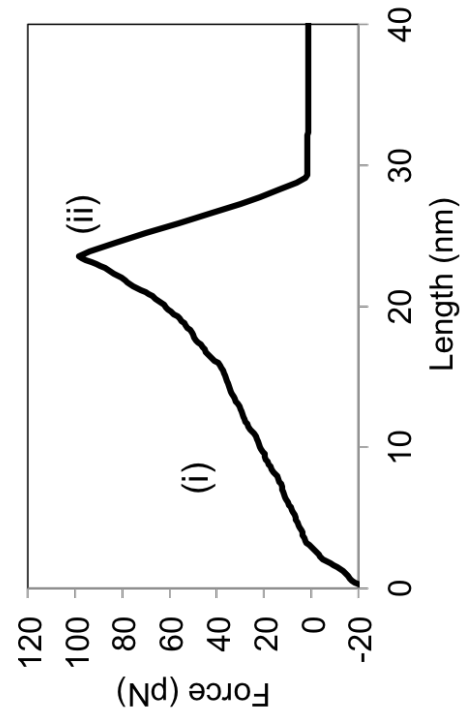
(vi)



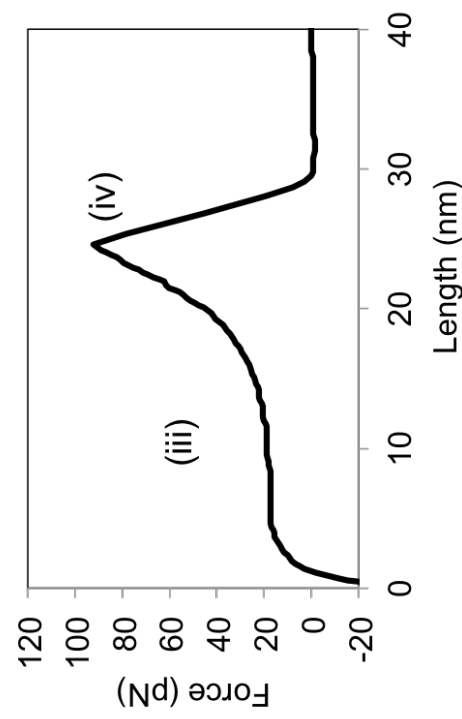
(vii)



(d)



(e)



(f)

